



ELSEVIER

Available online at www.sciencedirect.com

SCIENCE @ DIRECT®

Journal of Geodynamics 38 (2004) 451–460

JOURNAL OF
GEODYNAMICS

<http://www.elsevier.com/locate/jog>

Earth's free core nutation determined using C032 superconducting gravimeter at station Wuhan/China

He-Ping Sun^{a,*}, Gerhard Jentzsch^b, Jian-Qiao Xu^a, Hou-Ze Hsu^a,
Xiao-Dong Chen^a, Jiang-Cun Zhou^a

^a *Open Laboratory of Dynamics Geodesy, Institute of Geodesy and Geophysics,
Chinese Academy of Sciences, 54 Xu Dong road, 430077 Wuhan, PR China*

^b *Institute of Geosciences, University of Jena, Burgweg 11, D-07749, Jena, Germany*

Received 12 November 2003; received in revised form 23 June 2004; accepted 9 July 2004

Abstract

The long series tidal gravity observations from 1997 to 2002 recorded with C032 superconducting gravimeter (SG) at station Wuhan/China are used in order to study the Earth's geodynamics. The tidal gravity parameters are determined precisely using Eterna software package after careful data pre-processing. The Earth's free core nutation (FCN) resonant parameters (eigenperiods, quality factors and resonant strengths) are determined accurately. The results show the determined eigenperiod to be 431.0 sidereal days with an accuracy of $\pm 1.81\%$, the quality factor is a negative one as of -7002 , and the resonance strength can be explained by the elastic property of the Earth's mantle. The discrepancy of the eigenperiods when using various ocean models can amount to $\pm 1.8\%$. The 30 sidereal days difference between the determined eigenperiod in this paper and the one in theoretical computation given by Wahr and Bergen can be explained by the real dynamic ellipticity of the Earth's liquid core, i.e., it is about 5% larger than the one under the hydrostatic equilibrium assumption.

© 2004 Elsevier Ltd. All rights reserved.

1. Introduction

It is well known that compared to any spring gravimeter, the superconducting gravimeter (SG) has many excellent characteristics, including the wide measuring range, low noise level, and high stability

* Corresponding author. Tel.: +86 27 68881323; fax: +86 27 68881323.
E-mail address: heping@asch.whigg.ac.cn (H.-P. Sun).

and sensitivity (e.g., resolutions in the order of 10^{-3} μgal). The SG recordings with high sampling rates, especially after eliminating instrumental drifts and other systematic errors, can be used effectively to study the geodynamical signals such as Earth tides, the interactions between the solid Earth, ocean and atmosphere, the resonance effect of the free core nutation (FCN), the modes of the Earth's core, and gravity change due to tectonic motions and so on (Herring et al., 1991; Crossley et al., 1999; Kroner and Jentzsch, 1999; Ducarme et al., 2002; Sun et al., 2002; Xu et al., 2002).

The Wuhan SG-T004 observation started in 1985, and long series observations have been accumulated up to now. For the purpose to match the global geodynamics project (GGP) regulations, it was upgraded in 1997 via GWR company by equipping a new sensing unit and an improved dewar mounting and renamed as SG-C032. The instrument was then re-installed successfully in November 1997 at the geodynamics station about 25 km away from the city centre (coordinates: 30.52°N, 114.49°E and 89 m). The new data acquisition system developed by the German group (via G. Jentzsch, University of Jena) was also installed. The tidal gravity and pressure records with a 10 s interval are obtained from original 1 s sampling and sent to a 6.0 digital voltmeter. This report will describe the study of the Earth's FCN phenomena with some problems relating to the ocean tides and atmospheric pressure influence using the data from December 20, 1997 to December 31, 2002.

In order to convert effectively the digital output from volt into gravity unit in μgal , a FG5-112 absolute gravimeter is used. Two campaigns were carried out for this calibration studies (Sun et al., 2001). After applying for the corrections of the laser light speed, valid instrument height and adjustment height, the calibration factor was determined by using a least-square polynomial linear fit between the SG outputs and absolute gravity measurements. The data pre-processing is one of the most important steps for obtaining high precision gravity and air pressure data. The monthly records sampled at 10 s are pre-processed carefully by using Tsoft package (Vauterin, 1998). A moving window function is used to eliminate spurious signals as jumps, tares and spikes. The missing data due to power interruptions, earthquakes, refilling liquid helium are filled using a spline interpolation based on the synthetic tidal signals. The hourly sequence of the tidal gravity and pressure are then obtained using a remove–restore technique.

After this pre-processing, the tidal parameters are precisely determined by using Eterna 3.30 software package (Wenzel, 1996). The new tidal parameters determined are in good agreement with those obtained from the old series in 1985–1994 (Sun et al., 1998) with exhibiting a significant reduction of the station background noise and low instrumental drift. It is found that the precision of the main wave amplitude factors is as of 0.09% (O1) and 0.02% (M2), respectively. The tidal gravity residuals are obtained after removing the synthetic signals from the processed hourly series. The atmospheric gravity admittance is determined by using a regression technique between the residual gravity signals and the station pressure. The regression coefficients are found to be $-0.316 (\pm 0.009)$ $\mu\text{gal/hPa}$. With this coefficient, the pressure signals are removed before the tidal gravity parameters are determined.

2. Reduction of the oceanic loading signals

During the last decades, worldwide studies on the relationship between the deformation of the Earth and the effect of the ocean loading have been successfully carried out, as it is believed that they are important for the retrieval of the structural parameters in crust and upper mantle beneath gravity stations. It was demonstrated that the gravity observations on the Earth's surface are influenced by ocean loading

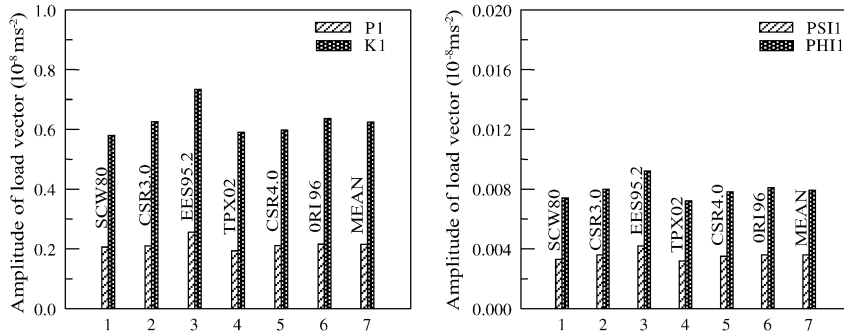


Fig. 1. Oceanic loading amplitudes for four diurnal waves near the FCN resonant frequency.

which can contribute to 10% of the total signal (Melchior and Francis, 1996). So, the gravity tidal data can be used as an important source to study the characteristics of the Earth’s deformation.

In recent years, the accuracy of the oceanic models has been improved significantly, thanks to the analysis of the precise measurements from Topex/Poseidon altimetry and as a result of parallel developments in numerical tidal modeling and data assimilation. It is important to remove the loading signals from tidal gravity parameters for a better determination of the FCN parameters. Based on a direct discrete convolution technique between the ocean tides and loading Green functions (Sun, 1992), the loading amplitude and phase (L , λ) for four main waves (P1, K1, PSI1 and PHI1) near the resonant frequency are calculated (Fig. 1). The global ocean models used in this study are the Schwiderski (SCW80) and the most recent global ocean models (PODAAC, 1999) as CSR3.0 (Eanes), FES95.2 (Le Provost et al.), TPX02 (Egbert), CSR4.0 (Eanes), ORI96 (Masumoto). Finally, the average one of the loading vectors for these models is taken into account in order to check a global influence. It is found that the loading amplitudes can reach 0.6 μgal for the K1 wave and 0.2 μgal for P1 wave. The loading vectors for another two small waves (PSI1 and PHI1) are obtained by using an interpolation technique in the frequency band (at $n\text{gal}$ level, Fig. 1). The core resonance phenomena on oceanic tides are taken into account during the interpolation process (Sun et al., 2003). The reduction efficiency of the tidal gravity residuals for both principal and small components is confirmed (Fig. 2).

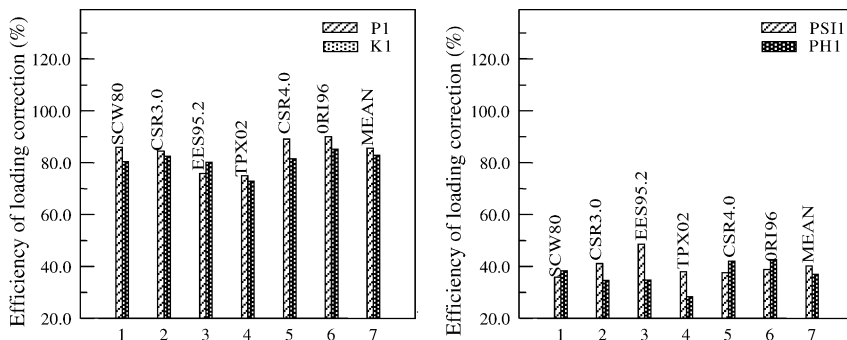


Fig. 2. Reduction efficiency of the tidal gravity residuals after loading correction.

Table 1
Tidal gravity residuals before and after oceanic loading correction

Model	P1 wave		K1 wave		PSI1 wave		PHI1 wave	
	μgal	($^{\circ}$)						
$B (B, \beta)$	0.2363	-27.78	0.7569	-28.54	0.0076	-61.98	0.0125	-0.93
$X_1 (X, \chi)$	0.0353	0.89	0.1769	-29.66	0.0049	-80.79	0.0076	32.06
$X_2 (X, \chi)$	0.0390	16.24	0.1679	5.54	0.0045	-80.43	0.0081	37.84
$X_3 (X, \chi)$	0.0571	75.99	0.1685	47.27	0.0039	-84.19	0.0081	46.44
$X_4 (X, \chi)$	0.0612	11.66	0.2378	10.05	0.0046	-74.47	0.0089	33.46
$X_5 (X, \chi)$	0.0281	-3.63	0.1759	-6.84	0.0048	-82.87	0.0071	33.84
$X_6 (X, \chi)$	0.0260	8.86	0.1494	3.98	0.0047	-83.47	0.0070	36.29
$X_7 (X, \chi)$	0.0360	22.14	0.1661	4.80	0.0046	-80.98	0.0078	36.72

Note: $B (B, \beta)$ the observed residual amplitudes and phases, $X_1 (X, \chi)$, $X_2 (X, \chi)$, $X_3 (X, \chi)$, $X_4 (X, \chi)$, $X_5 (X, \chi)$, $X_6 (X, \chi)$ represent the residual amplitudes and phases after oceanic loading correction when using the ocean model given as SCW80, CSR3.0, FES95.2, TPXO2, CSR4.0 and ORI96, respectively, $X_7 (X, \chi)$ the one after averaging loading correction of six ocean models.

Based on the (L, λ) given in Fig. 1, the tidal gravity residuals and parameters for waves near the resonant frequency are corrected. Table 1 shows the residual amplitude and phase before (B, β) and after (X, χ) oceanic loading correction. Averaging those loading corrected residuals, it is found that the residual amplitudes are reduced significantly from 0.236 to 0.036 μgal (P1), from 0.757 to 0.166 μgal (K1), from 0.008 to 0.005 μgal (PSI1) and from 0.013 to 0.008 μgal (PHI1). The average reduction efficiency when carrying out the loading correction are given as 85.6% (P1), 82.84% (K1), 40.1% (PSI1), and 36.9% (PHI1) respectively (see Fig. 2). It shows the effectiveness of the loading correction for principal waves and a lesser effectiveness for small waves. However, this reduction of the residuals for those small waves is very useful for improving the accuracy of the FCN parameters. Table 2 shows the tidal gravity amplitude factors and phase differences before $(\delta, \Delta\varphi)$ and after $(\delta', \Delta\varphi')$ loading correction. Compared to the Sun-Xu-Ducarme (SXD) experimental tidal gravity model determined with tidal gravity observations in

Table 2
Tidal gravity amplitude factors and phase lags before and after ocean loading correction

Models	P1 wave		K1 wave		PSI1 wave		PHI1 wave	
	μgal	($^{\circ}$)						
$\delta (\delta, \Delta\varphi)$	1.1658	-0.43	1.1528	-0.47	1.2790	-1.00	1.1928	-0.02
$\delta_1 (\delta', \Delta\varphi')$	1.1520	0.002	1.1393	-0.12	1.2696	-0.73	1.1817	0.36
$\delta_2 (\delta', \Delta\varphi')$	1.1522	0.04	1.1397	0.02	1.2695	-0.67	1.1816	0.44
$\delta_3 (\delta', \Delta\varphi')$	1.1503	0.22	1.1383	0.16	1.2683	-0.59	1.1802	0.53
$\delta_4 (\delta', \Delta\varphi')$	1.1540	0.05	1.1414	0.05	1.2711	-0.67	1.1835	0.44
$\delta_5 (\delta', \Delta\varphi')$	1.1514	-0.01	1.1399	-0.03	1.2690	-0.72	1.1807	0.35
$\delta_6 (\delta', \Delta\varphi')$	1.1513	0.02	1.1392	0.01	1.2688	-0.71	1.1803	0.37
$\delta_7 (\delta', \Delta\varphi')$	1.1519	0.05	1.1396	0.02	1.2694	-0.68	1.1813	0.41

Note: $\delta (\delta, \Delta\varphi)$ the observed amplitude factors and phase lags, $\delta_1 (\delta', \Delta\varphi')$, $\delta_2 (\delta', \Delta\varphi')$, $\delta_3 (\delta', \Delta\varphi')$, $\delta_4 (\delta', \Delta\varphi')$, $\delta_5 (\delta', \Delta\varphi')$, $\delta_6 (\delta', \Delta\varphi')$ represent the amplitude factors and phase lags after loading correction when using various ocean models as SCW80, CSR3.0, FES95.2, TPXO2, CSR4.0 and ORI96, respectively, $\delta_7 (\delta', \Delta\varphi')$ the one after averaging loading correction of six ocean models.

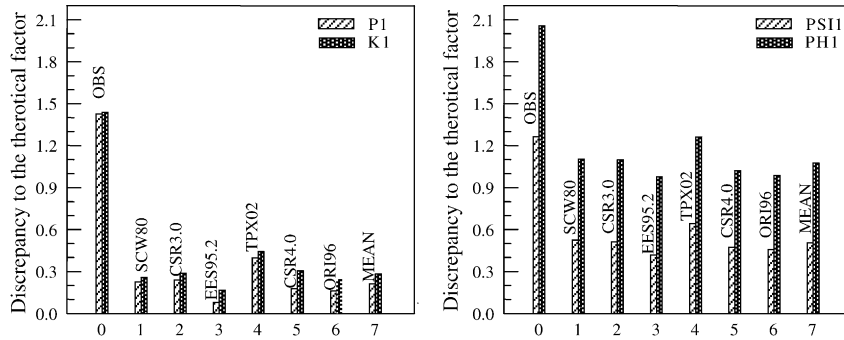


Fig. 3. Discrepancy between amplitude factors before (after) loading correction and theoretical model.

GGP network with considering the FCN phenomena (Sun et al., 2003), the discrepancy is reduced from 1.425 to 0.213% (P1), from 1.437 to 0.283% (K1), from 1.263 to 0.504 (PS11) and from 2.056 to 1.074 (PS11), they can be seen in Fig. 3.

From Tables 1 and 2, it is found that although applying the ocean loading corrections, the residual disturbances still remain, which obviously are produced by insufficient correction, or induced by other local perturbations, as the change of regional pressure, of temperature, of underground water and so on. The lateral heterogeneity of the Earth not yet included in tidal model may also increase such discrepancies.

3. Determination of the FCN resonant parameters

The Earth’s FCN is an important retrograde free nutation normal mode, caused by the interaction of a solid elastic mantle and a fluid core in a rotating elliptical Earth with a slightly elliptical deformable core-mantle boundary (CMB). The FCN resonance has an eigenperiod T_{FCN} close to one sidereal day (sd) in the mantle reference frame and approximately 435 sd in the space reference frame (Hinderer et al., 1993). Based on an given Earth’s model, the eigenperiod of the FCN can be predicted theoretically, it is in the range from 455.8 to 467.4 sidereal days by means of analytical or numerical integration to angular momentum equations of the Earth (Wahr and Bergen, 1986). Based on the least-square fit of the tidal gravity data to a damped harmonic oscillator, the same procedures as Defraigne et al. (1994) are employed for determining the FCN resonance parameters.

It is known that in diurnal band, the theoretical amplitude factor $\delta th(\sigma)$ can be expressed as the sum of the normal amplitude factor δ_0 (the part independent from frequency) and the one as a function of the normal tidal frequency σ and the FCN resonant frequency $\bar{\sigma}_{FCN}$ given as

$$\delta th(\sigma) = \delta_0 + \frac{\bar{A}}{\sigma - \bar{\sigma}_{FCN}}, \quad (1)$$

where

$$\delta_0 = 1 + h_0 - \frac{3}{2}k_0, \quad \bar{A} = - \left(\frac{A}{A_m} \right) \left(h_1 - \frac{3}{2}k_1 \right) \left(\alpha - q_0 \frac{h^c}{2} \right) \Omega, \quad (2)$$

where h_0 and k_0 are the classical Love numbers, δ_0 is not influenced by the resonance, \bar{A} is the resonant strength relating to the geometric shape of the Earth and the rheology properties of the mantle. The h_1

and k_1 are the internal pressure Love numbers, h^c is the secular Love number, A and A_m are the equatorial moments of inertia of the entire Earth and the solid mantle, α is the dynamic ellipticity of the Earth, q_0 is the ratio of the centrifugal force to gravity on the equator, Ω the sidereal frequency of the Earth's rotation. For an elastic Earth model, \bar{A} can be described as a real one, however, for an anelastic model, the resonance strength and the FCN eigenfrequency are described as a complex with a very small imaginary part, denoting as

$$\bar{A} = A_r + iA_i, \quad \bar{\sigma}_{\text{FCN}} = \sigma_r + i\sigma_i, \quad (3)$$

Therefore, the eigenperiod and quality factor are given as $T_{\text{FCN}} = \Omega/(\sigma_r + \Omega)$ and $Q = \sigma_r/2\sigma_i$. The studies show that in the diurnal band, the wave O1 occupies a largest amplitude, high ratio of signal to noise and high observation accuracy. Considering its frequency is far away from the resonant one, it is less influenced by the FCN resonance (at the order of 10^{-4}), therefore, it can be referred as a reference in the computing procedure of the FCN. The fitting equations can be deduced by modeling the observed complex diurnal tidal gravity parameter to theoretical ones given in expression (1) and removing the signals of wave O1.

$$\delta(\sigma, j) - \delta(\text{O1}, j) = \frac{A_r + iA_i}{\sigma - (\sigma_r + i\sigma_i)} - \frac{A_r + iA_i}{\sigma(\text{O1}) - (\sigma_r + i\sigma_i)} \quad (4)$$

where j stands for the series number of stations. It is found that the Eq. (4) is obviously non-linear, to solve these equations when n tidal waves are included, it is necessary for us to minimize the error function χ^2 by using the Marquadt's algorithm of linearized iteration and modification

$$\chi^2 = \sum_{\sigma, j} \omega(\sigma, j) \left| [\delta(\sigma, j) - \delta(\text{O1}, j)] - \left[\frac{A_r + iA_i}{\sigma - (\sigma_r + i\sigma_i)} - \frac{A_r + iA_i}{\sigma(\text{O1}) - (\sigma_r + i\sigma_i)} \right] \right|^2, \quad (5)$$

with $\omega(\sigma, j) = 1/\varepsilon(\sigma, j)$ the weight function, where $\varepsilon(\sigma, j)$ is the standard deviation of the amplitude factor of a tidal wave with frequency σ at the j th station.

By using the loading corrected tidal gravity parameters in diurnal band as given in Table 2 and Eq. (4), the resonant parameters of the FCN, i.e., the eigenperiod, the quality factor Q and the resonant strength are calculated. The corresponding numerical results (eigenperiods, quality factor Q value and resonant strengths) are given in Table 3, the value in brackets represent error range. It is found that resonant parameters differ from one to another when using different oceanic models. The maximum discrepancy can reach $\pm 1.80\%$. The determined eigenperiods are found to be 427.7 sd with an error of $\pm 1.58\%$ (SCW80), 436.4 sd with an error of $\pm 2.91\%$ (CSR3.0), 437.7 sd with an error of $\pm 2.62\%$ (FES952), 421.6 sd with an error of $\pm 1.62\%$ (TPXO2), 431.8 sd with an error of $\pm 1.86\%$ (CSR4.0), 435.9 sd with an error of $\pm 2.11\%$ (ORI96) respectively. In order to consider the local ocean characteristics and other local influence, the average loading effect of six different global oceanic tidal models is considered. The determined eigenperiod is given as 431.0 sd with an error of $\pm 1.81\%$. It is found that the error is smaller when using CSR4.0 compared to CSR3.0 which proves the accuracy of the CSR4.0 to be significantly improved. The FCN eigenperiods are also computed for the comparison when using the SG data after loading correction with various ocean models at station Boulder/USA (from January 10, 1998 to May 31, 2001) (Table 3). It is found that the eigenperiod is in the range from 427.4 to 432.0 sd, and it is 428.9 sd with an error of $\pm 1.1\%$ when using an average loading vector. The resonant parameters when stacking

Table 3
FCN Resonance parameters determined using Wuhan SG observations

Station	Model	T_{FCN} (sd)	Q value	$A_r \times 10^{-4}$ (°/h)	$A_i \times 10^{-4}$ (°/h)
Wuhan	SCW80	427.7 (421.0, 434.5)	−5140 (−8292, −3725)	−6.48 (0.30)	−0.07 (0.30)
	CSR3.0	436.4 (424.1, 449.5)	−124483 (8011, −7099)	−6.77 (0.50)	1.28 (0.50)
	FES952	437.7 (426.3, 449.6)	−9493 (86223, −4499)	−7.03 (0.44)	0.77 (0.44)
	TPXO2	421.6 (414.9, 428.5)	−4157 (−6101, −3153)	−6.13 (0.33)	−0.46 (0.33)
	CSR4.0	431.8 (423.9, 439.9)	−6584 (−15070, −4212)	−6.66 (0.33)	0.32 (0.33)
	ORI96	435.9 (426.9, 445.3)	−8935 (−64557, −4800)	−6.90 (0.36)	0.66 (0.36)
	Mean	431.0 (423.3, 438.9)	−7002 (−16921, −4415)	−6.62 (0.33)	0.37 (0.33)
	Boulder	SCW80	432.0 (414.4, 451.1)	6552 (3137, 73940)	−6.45 (0.68)
CSR3.0		425.0 (411.7, 439.2)	5297 (2936, 27056)	−6.01 (0.60)	−0.18 (0.60)
FES952		431.7 (411.0, 454.6)	3940 (2202, 18683)	−6.59 (0.64)	0.01 (0.63)
TPXO2		429.9 (415.8, 445.0)	6641 (3249, −151656)	−6.29 (0.59)	−0.58 (0.59)
CSR4.0		427.6 (413.0, 443.2)	4895 (2711, 25157)	−6.25 (0.63)	−0.19 (0.63)
ORI96		427.4 (413.4, 442.4)	6586 (3225, −157066)	−6.12 (0.61)	−0.52 (0.61)
Mean		428.9 (424.3, 433.6)	5453 (4274, 7531)	−6.29 (0.19)	−0.34 (0.19)
Global (20 stations)		SCW80	432.1 (428.8, 435.4)	12760 (8805, 23167)	−6.58 (0.14)
	CSR3.0	428.6 (425.5, 431.7)	−28503 (14544, 70898)	−6.29 (0.13)	−0.19 (0.13)
	FES95.2	432.9 (429.9, 435.8)	17485 (11279, 38867)	−6.64 (0.12)	−0.05 (0.12)
	TPXO2	434.7 (431.4, 438.1)	−60940 (−191589, 69709)	−6.71 (0.13)	−0.56 (0.13)
	CSR4.0	425.9 (423.1, 428.8)	16520 (10717, 33592)	−6.12 (0.13)	0.02 (0.13)
	ORI96	434.6 (431.3, 438.0)	9378 (7053, 14031)	−6.77 (0.13)	0.25 (0.13)
	Stacking	429.9 (427.2, 432.7)	20769 (12898, 53289)	−6.41 (0.12)	−0.10 (0.12)

Note: Global means the results obtained when stacking the SG tidal gravity data from 20 stations in the GGP network from Stations Bandung, Brussels, Boulder, Brasimone, Cantley, Canberra, Esashi, Kyoto, Matsushiro, Membach, Metsahovi, Moxa (2 series), Pecny (spring gravimeter), Potsdam, Strasbourg (2 series), Sutherland (2 series), Syowa, Vienna, Wettzell (3 series), Wuhan (2 series) (see Ducarme et al., 2003).

the global tidal gravity observations at 20 stations in the GGP network using various ocean models are also listed in Table 3 (for details see Ducarme et al., 2003).

Our results show that the resonant eigenperiods T_{FCN} (431.0 for Wuhan, 428.9 for Boulder and 429.9 for global) determined when using the SG observations are very close to the one (429.5 sd) obtained from the theoretical computations (Dehant et al., 1999) and the one (430.04 sd) obtained when using VLBI data with considering the electro-magnetic coupling force at the core-mantle boundary (Mathews et al., 2002). The discrepancy does not exceed 0.3%. However, it is found that there exists a discrepancy when comparing these results with those obtained in early studies. Furthermore, it should be pointed out that the discrepancy is as large as 30 sd when comparing experimental results with those from early theoretical computations assuming hydrostatic equilibrium (Wahr and Bergen, 1986). Therefore, it is necessary for us to investigate the corresponding reasons.

As a matter of fact, the early studies show that the FCN resonant parameters depend mainly on the Earth's structural, physical and mechanical properties. Based on an Earth's model with an elastic solid mantle, a fluid outer core and an elastic solid inner core, the analytical expression of the FCN

eigenfrequency σ_{FCN} ($\sigma_{\text{FCN}} = 1/T_{\text{FCN}}$) can be given approximately as

$$\sigma_{\text{FCN}} = - \left[1 + \frac{A - A_{\text{I}}}{A_{\text{m}}} (e_{\text{f}} - \beta) \right] \Omega, \quad (6)$$

where e_{f} is the dynamic ellipticity of the Earth's liquid core (at the order of 10^{-3}), β is a small parameter describing the elastic deformation of the mantle (at the order of 6.27×10^{-4}), A , A_{I} and A_{m} are the equatorial inertia moments of the whole Earth, mantle and solid inner core. Among them A_{I} is only at the level 10^{-4} of the A . The earlier theoretical studies indicate that in assumption of the hydrostatic equilibrium, only a few sd discrepancy on the T_{FCN} for various Earth models is found. The present discrepancies between the observed tidal gravity amplitude factors and those given in theoretical tidal modelling are less than 0.4% which implies that the real Earth's deformation can well approximated by the recent Earth's deformation theory. Therefore when having measured with high precision FCN eigenfrequency, from formula (6), the dynamic ellipticity of the Earth's fluid core e_{f} can then be calculated. Based on our numerical results, the reasonable explanation to the 30 sd less of the observed eigenperiod than the one in theoretical computation is that the real dynamic ellipticity of the Earth's liquid core is about 5% larger than the one given under the hydrostatic equilibrium assumption.

The determined quality factor Q values are negative and differ significantly depending on the used ocean tidal model. They are given as -5140 (SCW80), -124483 (CSR3.0), -9493 (FES952), -4157 (TPXO2), -6584 (CSR4.0) and -8935 (ORI96). The final one when averaging the loading vectors of six oceanic models is -7002 . Also, the different Q values with positive sign are obtained at station Boulder when using various ocean models, but the magnitude of the Q value is of the same order. It is found that when stacking the global SG data, the Q value is 20769, about one order larger than the one from a single station. The observed Q values can't be interpreted only by the inelasticity of the mantle, and negative value may reflect the Earth's rheology property. In the theoretical modeling, the Q value arrives in amount than 78000 (Wahr and Bergen, 1986). If a layer with high viscosity at the bottom of the mantle or a conducting layer at the top of the liquid core is taken into account, the electro-magnetic or viscous coupling between the mantle and core will play a very significant role to Q value. Therefore, a low Q value may relate to the local environmental perturbation and the properties of the Earth beneath gravity station.

The fitted FCN complex resonance strength is $(-6.62 \times 10^{-4}, 0.37 \times 10^{-4})^{\circ}/\text{h}$ for station Wuhan and is $(-6.29 \times 10^{-4}, 0.34 \times 10^{-4})^{\circ}/\text{h}$ for station Boulder, which are in agreement with the one from theoretical computations based on an inelastic Earth models (Wahr and Bergen, 1986). In other words, the resonance strength determined in our study can be well interpreted by using the mantle inelasticity of the Earth.

The significant agreement and disagreement with previous studies and the theoretical computations imply that the fitted resonance parameters using the data series from a single station strongly depend on the oceanic models. In other words, the uncertainty in oceanic models will lead to the discrepancies in determination of the FCN parameters. So to select the best ocean model is of great importance for the FCN determination. Also the analysis shows that the oceanic and barometric pressure influences are the main error sources for the FCN parameters. In addition to these, the errors of the phase lags can be responsible for a biased Q .

4. Discussions and conclusions

The tidal gravity parameters based on Wuhan SG observations from 1997 to 2002 are determined precisely based on a standard Eterna package after a careful data pre-processing and station pressure correction. It is found that the small instrument drift and the significant reduction of the site background noise allow us to estimate high accuracy gravimetric factors and to check more optimally the various oceanic models. Due to the low site background noise and precise loading correction, the inversion of the FCN resonant parameters reveals the results in accordance with previous studies given by international colleagues. The discrepancy among the determined eigenperiods when using various oceanic models differs by $\pm 1.8\%$. The 30 sd eigenperiod difference between experimental result and early theoretical computation of Wahr and Bergen is that the real dynamic ellipticity of the Earth's liquid core is about 5% larger than the one given under the hydrostatic equilibrium assumption. Therefore, the gravity is an important technique to obtain the real dynamic ellipticity of the Earth's liquid core independent from seismology. However, the significant difference among the quality factor Q values when using various ocean models should be further investigated, a stacking of the SG data in the GGP network is necessary for reducing as possible the local environmental influence and background noises in determination of the FCN parameters. A further study on the influence of the regional pressure change, of temperature, of underground water will be carried out for a better retrieval of the FCN parameters from the global SG measurements.

Acknowledgement

This work is supported jointly by the Knowledge Innovation Project and the Hundred Talents Program, Chinese Academy of Sciences (KZCX3-SW-131), the National Natural Science Foundation of China (No. 40374029) and the Key International Cooperative Project, Ministry of the Sciences and Technology of China (2002CB713904).

References

- Crossley, D., Hinderer, J., Casula, G., Francis, O., Hsu, H.-T., Imanishi, Y., Jentzsch, G., Kääriäinen, J., Merriam, J., Meurers, B., Neumeyer, J., Richter, B., Shibuya, K., Sato, T., van Dam, T., 1999. Network of superconducting gravimeters benefits a number of disciplines. *Eos, Trans., Am. Geophys. Union* 80 (11), 121, 125–126.
- Defraigne, P., Dehant, V., Hinderer, J., 1994. Staking gravity tide measurements and nutation observations in order to determine the complex eigenfrequency of nearly diurnal free wobble. *J. Geophys. Res.* 99 (B5), 9203–9213.
- Dehant, V., Defraigne, P., Wahr, J., 1999. Tides for a convective Earth. *J. Geophys. Res.* 104 (B1), 1035–1058.
- Ducarme, B., Sun, H.-P., Xu, J.Q., 2002. New investigation of tidal gravity results from the GGP network. *Bull. d'Inf. Marees Terrestres.* 136, 10761–10775.
- Ducarme, B., Sun, H.-P., Xu, J.Q., 2003. Tidal gravity and tidal loading results from the GGP network, physics of the Earth and planetary interior. *Phys. Earth Planet. Interior*, submitted for publication.
- Herring, T.B., Buffett, P., Mathews, S., Shapiro, I., 1991. Forced nutations of the Earth: influence of inner core dynamics, a very long baseline Interferometry data analysis. *J. Geophys. Res.* 96, 8243–8257.
- Hinderer, J., Crossley, D., Xu, H., 1993. The accuracy of tidal gravimetric factors and nearly diurnal free wobble resonance parameters in superconducting gravimetry. In: Hsu, H.T. (Ed.), *Proceedings of the 12th International Symposium on Earth Tides*. Science Press, Beijing, August 4–8, 1993, pp. 289–297.

- Kroner, C., Jentzsch, G., 1999. Comparison of different barometric pressure reductions for gravity data and resulting consequences. *Phys. Earth Planet. Interior* 115, 205–218.
- Mathews, P.M., Herring, T.A., Buffett, B.A., 2002. Modeling of nutation-precession: new nutation series for nonrigid Earth and insights into the Earth's interior. *J. Geophys. Res.* 107 (B4): ETG3-1-3-30.
- Melchior, P., Francis, O., 1996. Comparison of recent ocean tidal models using ground based tidal gravity measurements. *Marine Geodesy* 19, 291–330.
- PODAAC., 1999. A collection of the global ocean tide models. JPL Physical Oceanography DAAC Data Distribution, USA, pp. 1–25.
- Sun, H.-P., 1992. Comprehensive researches for the effect of the ocean loading on gravity observations in the Western Pacific area. *Bull. d'Inf. Marees Terrestres.* 113, 8271–9292.
- Sun, H.-P., Chen, X.-D., Hsu, H.-Z., Wang, Y., 2001. Accurate determination of calibration factor for tidal gravity observation of a GWR-superconducting gravimeter. *Acta Seismologica Sinica* 14 (6), 692–700.
- Sun, H.-P., Ducarme, B., Hinderer, J., Hsu, H.-T., 1998. Intercomparison of the (non-) tidal gravity observations with superconducting gravimeters at stations Wuhan, Brussels and Strasbourg. In: Ducarme, B., Paquet, P. (Eds.), *Proceedings of the 13th International Symposium on Earth Tides. 20–24 July 1997. Série Géophysique Royal Observatory of Belgium, Brussels*, pp. 455–462.
- Sun, H.-P., Hsu, H.-Z., Jentzsch, G., Xu, J.-Q., 2002. Tidal gravity observations obtained with superconducting gravimeter and its application to geodynamics at Wuhan/China. *J. Geodyn.* 33 (1–2), 187–198.
- Sun, H.-P., Xu, J.-Q., Ducarme, B., 2003. Experimental earth tidal models in considering nearly diurnal free wobble of the Earth's liquid core. *Chin. Sci. Bull.* 48 (9), 935–940.
- Vauterin, P., 1998. Tsoft: graphical and interactive software for the analysis of Earth tide data. In: Paquet, P., Ducarme, B. (Eds.), *Proceedings of the 13th International Symposium on Earth tides, Brussels[C], Geophysical Series. Royal Observatory of Belgium*, pp. 481–486.
- Wahr, J.M., Bergen, Z., 1986. The effects of mantle anelasticity on nutations, earth tides, and tidal variations in rotation rate. *Geophys. J. R. Astr. Soc.* 87, 633–668.
- Wenzel, H.G., 1996. The nanogal software: Earth tide data processing package Eterna3.30. *Bull. d'Inf. Marees Terrestres.* 124, 9425–9439.
- Xu, J.-Q., Sun, H.-P., Luo, S.-C., 2002. Study of the Earth's free core nutation by tidal gravity data recorded with international superconducting gravimeters. *Sci. China (Series D)* 45 (4), 337.